Validation Test Design for a Nonlinear Model Developed from Limit Cycle Data

Wayne J. Dunstan, Department of Mechanical & Aerospace Engineering,
University of California San Diego, La Jolla CA 92093-0411, USA. wdunstan@ucsd.edu

Robert R. Bitmead[1], Department of Mechanical & Aerospace Engineering,
University of California San Diego, La Jolla CA 92093-0411, USA. rbitmead@ucsd.edu

Sergio M. Savaresi, Dipartimento di Elettronica e Informazione, Politecnico di Milano,
Piazza L. da Vinci, 32, 20133 Milan, Italy. savaresi@elet.polimi.it

Abstract

This paper details an example of experiment design for validation of a nonlinear model arising in the limit cycling behavior of lean, premixed combustion. The validation problem is important because of the poor information content of the periodic limit cycle data and the challenge is to provide a practically feasible, small excitation to the loop to improve identifiability and to provide qualitative tests of model performance. We examine this problem by considering the nonlinear dynamics of the model class and feasible excitation mechanisms.

1 Introduction

In a recent paper [SBD2K], the authors fitted a nonlinear model describing the limit cycling behavior of a burning flame in a lean, premixed combustor as might be found in a gas turbine or jet engine operating at very low equivalence (fuel-to-air) ratios (ϕ). The underlying model structure is based on a thermo-acoustic combustion model proposed by Peracchio and Proscia [PP98] which captures the large scale effects in the combustor. The model fitting used data from combustion experiments conducted on an experimental rig at United Technology Research Center (UTRC) [MJC+98]. Peracchio and Proscia [PP98] developed the first approaches to the model fitting, which were later amplified and extended in [MJC+98]. In this paper we explore the design of validation experiments which might be applied to test the veracity of the identified system.

As shall be seen, the data from the original experiment are quite poor in terms of parameter identifiability for a model of this complexity. As a result of this information paucity of the experimental data, we now look to design subsequent practical experiments which might provide more information towards the model validation/invalidation.

The nonlinear model that we fit necessarily must capture the limit cycle effect and, hence, exhibit non-linear closed-loop dynamics. Exciting non-linear oscillations with external signals introduces the prospect of exceedingly complicated behavior [GH96]. Our aims are mostly qualitative in nature: to improve signal identifiability via excitation injection; to explore the induced occurrence of new effects and phenomena; to understand the implied prospects for closed-loop control of the oscillation. To appreciate these issues, we appeal to the results on the excitation of nonlinear systems with multiple attractors. Underpinning our selection of excitation signals for these validation tests is the requirement that they be physically realizable in experiments using standard actuation techniques.

2 Experimental Data and Thermo-acoustic Model

The data were obtained from the UTRC/DARPA Single Nozzle Rig Experiment and consist of six unexcited closed-loop experiments conducted at different equivalence ratios within the region where the system is limit cycling. For each experiment the pressure, p_t, and heat release rate, q_t, were sampled at 5000Hz and 16000 samples were logged during the non-transient phase of the limit cycle.

Figure 1 shows the pressure data (p_t) from Experiment 1 (ϕ=0.56) in the time and frequency domains. From a qualitative analysis of the p_t and q_t data over the six experiments, the following preliminary conclusions can be drawn:

• The data is almost periodic. It is dominated by sinusoids at 210Hz and 740Hz, plus harmonics of 210Hz and some small broad-band noise component. Note that it is almost periodic (and not periodic) because the 210Hz

[1]This work was supported in part by the NSF under Grant ECS-0070146000

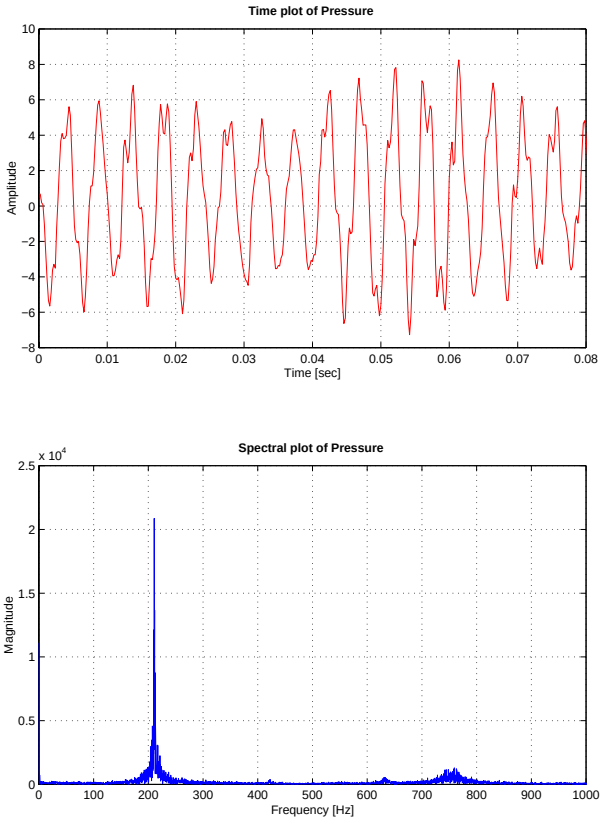

Figure 1: Time and spectral plots of the pressure data for Experiment 1

and 740Hz signals are not harmonically related.
•The 210Hz mode shifts with ϕ while the 740Hz signal does not.
•The q_t signal is deficient of high frequency components because the measuring device exhibits a low pass filtering effect. The model developed in [SBD2K] is shown in Figure 2.

3 Nonlinear System Identification

The model in Figure 2 is parametrized by five parameters$(\tau, M, N, \xi, \omega)$ which are non-linearly related. However, as illustrated in Figure 1, the spectral content of p_t is supported by two frequencies well and at most four frequencies in total. The spectral content of q_t is even more deficient because of the low pass filtering. Working around the loop of the model in Figure 2 we identify the following parameters.
• **Time delay** τ is identified by comparing the phases of the fundamental harmonics of the q_t and p_t signals. The differentiator and nonlinearity add $\frac{3\pi}{2}^c$ to the phase of p_t, with the remainder of the phase difference being due to the delay. The lowpass filter (LPF) applying to q rolls off outside the bandwidth of the fundamental harmonic. This results in $\tau = 3.47$msec, constant for all ϕ.

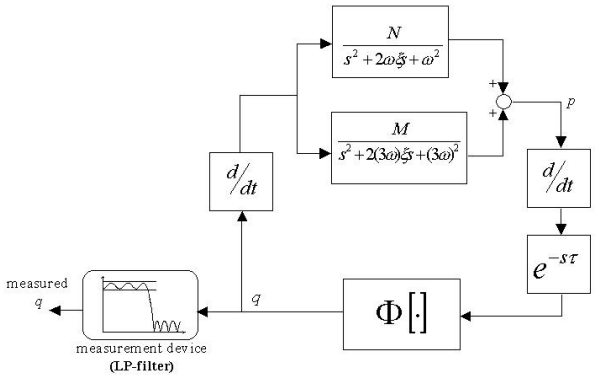

Figure 2: Limit cycling combustion model.

• **Memoryless nonlinearity** Φ is charted by reconstructing the input signal to the nonlinearity by mapping each periodic component in p_t to reproduce the input to Φ. With this signal and q_t, we plot the nonlinearity. The identified $\Phi[\cdot]$ for Experiment 1 is a negative slope saturation with a DC offset, shown in Figure 3. The slope and range of Φ vary with equivalence ratio, ϕ, i.e. with experiment, but maintain a similar form.
• **Coupled oscillators** are fitted using the succession of permissible loop phase values at the fundamental oscillating frequency over the range of six experiments. The structure is taken to be a fundamental oscillator plus a third harmonic oscillator, operating at the natural frequency and damping ratio of the acoustics of the combustion chamber (an *organ pipe* acoustic model). The identified oscillators have values of ω=206Hz, $\xi = 0.2\text{sec}^{-1}$, $N = 1$, $M = 1$. Note that ω **does not** equal the frequency of the fundamental oscillation in the data.

Although we can identify the set of five parameters of the linear part of the model, we have little confidence in their accuracy. The spectral content of the data is low (or at least poorly conditioned), the variations between experiments is small, and we are trying to use this data to fit five parameters. We are concerned about the quality of the fit, particularly for M, N, ξ and ω. When identification is conducted over different data sets for varying ϕ, it becomes difficult to distinguish changes in $\Phi[\cdot]$ and changes in the parameters. One of our aims here is to explore excitation of the loop to improve signal quality from an identifiability perspective. But before new experiments can be posed, the current model must be fully explored so as determine how to design experiments such that they might yield useful discriminating information.

4 Properties of the model

The identified model from Experiment 1 is depicted in Figure 3, showing the memoryless nonlinearity, and Figure 4 which shows the Nyquist diagram for the complete linear forward path from the output of the nonlinearity to its input. Notice the real axis crossings in

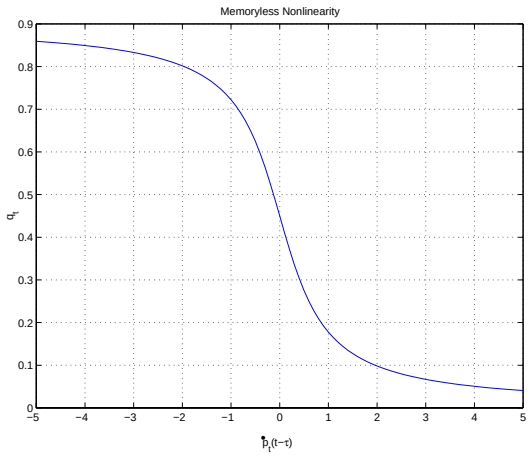

Figure 3: Memoryless nonlinearity

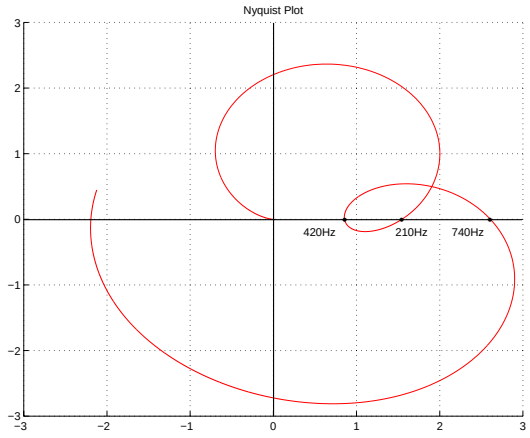

Figure 4: Nyquist plot of the linear section.

Figure 4. This would indicate possible oscillations at 210Hz, 420Hz and 740Hz. The fact that a model built for harmonic balancing at the fundamental frequency of the limit cycle is able to predict the possible existence of the non-harmonic 740Hz component is very surprising.

4.1 Describing Function Analysis

We can attempt to use describing function analysis even though this system does not adhere strictly to some of the formal prerequisites[1]. Figure 5 shows the real axis section of the Nyquist plot from Figure 4, along with the describing function $\Psi(a)$. (Note the nonlinearity's

[1] Most notably, the linear part of the system should be predominantly low pass, but also the system should be finite-dimensional and $\Phi[\cdot]$ should be odd.

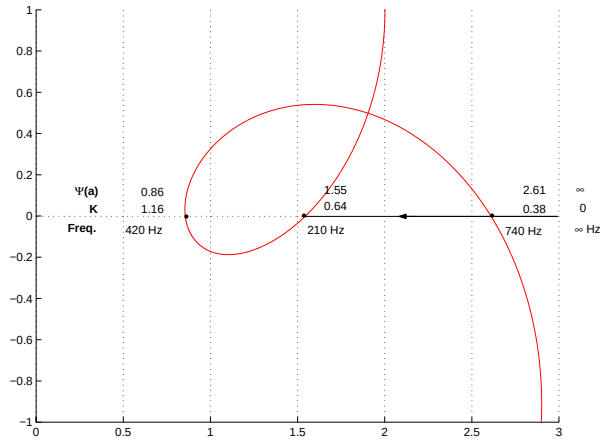

Figure 5: Zoom in of Figure 4 and the describing function of Φ with gain K.

gain $K = \Psi^{-1}(a)$ where a is the amplitude of sinusoid applied to the input of the nonlinearity.) Since the nonlinearity is memoryless and has negative slope, its describing function lies on the positive real axis. For small signals the gain of the non-linearity is K=0.64, which corresponds to $\Psi(a)$=1.55, which occurs at the 210Hz intersection point. For large signals the non-linearity's gain saturates and in the limit tends to zero. Thus the gain of the non-linearity varies between $0 < K < 1.55$ as $\infty > \Psi(a) > 0.64$. If one were able directly to alter the nonlinear gain, describing function methods would indicate that as the gain of the non-linearity increases from zero, the 740Hz oscillation should appear first, followed by the 210Hz, followed by 420Hz oscillation. It would also indicate that the 740Hz mode should be stable with the 210Hz and 420Hz modes unstable and probably saddle point stable, i.e. hyperbolic.

4.2 Simulation

Simulating the model with the above parameters produces p_t with a spectrum concentrated at 210Hz. The 740Hz oscillation is absent. The following is a summary of the observations while increasing K from zero:

- At $K = 0(\Psi(a) = \infty)$ no stable oscillations are present. There are 210Hz and 740Hz signals appearing as transients which quickly decay to zero.
- At $K = 0.38(\Psi(a) = 2.61)$ the 740Hz stable oscillation appears and increases in magnitude with increasing K. The 210Hz signal is present as a transient and decays to zero.
- At $K = 0.64(\Psi(a) = 1.55)$ the 210Hz stable stable oscillation appears and increases in magnitude with increasing K. The 740Hz oscillation is no longer present.
- For $K > 0.64(\Psi(a) < 1.55)$ The 210Hz oscillator remains stable, and harmonics start appearing. Note though that the 2^{nd} harmonic does not appear at all, regardless of the gain.

Describing function analysis correctly predicts the oc-

currence of the 210Hz and 740Hz oscillations at the gains detailed in the above summary, (see Figure 5). However it incorrectly describes the stability of the 210Hz oscillation.

We may turn to bifurcation theory [GH96] in an attempt to explain the evolution of stability properties witnessed. The system appears to be undergoing a Hopf Bifurcation at the K=0.38 point, followed by a destabilizing flip bifurcation at K=0.64. What occurs at K=1.16 on the Nyquist plot, shown in Figure 5, is not obvious, but from the simulations it does not yield a stable limit cycle at 420Hz. This bifurcation description is speculative, and would require further analysis of the Jacobian before confident statements could be made. But until the model is further validated, it is not sensible to perform the detailed calculations.

4.3 Phase Plane Analysis – Multiple Attractors

Consider the system response for K=0.39 ($\Psi(a)$=2.56), which is shown as a spectrogram in Figure 6. At the

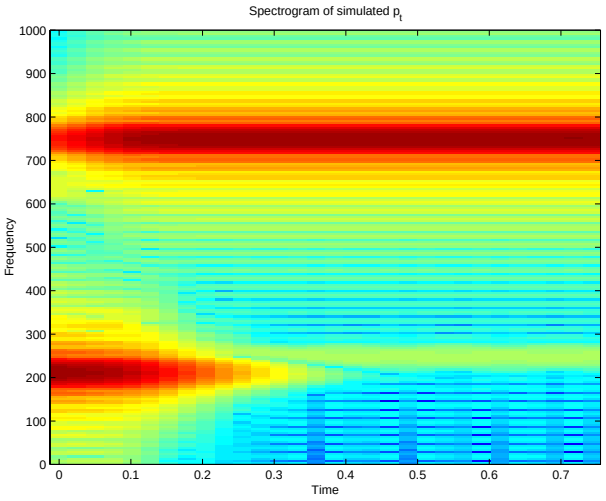

Figure 6: Spectrogram of simulated p_t K=0.39.

beginning of the response both 210Hz and 740Hz signals are present however, after ≈400msec the 740Hz remains and the 210Hz signal disappears.

This indicates that, for this gain, the 740Hz limit cycle is stable but there exists either a resonant mode near 210Hz or an unstable orbit at this frequency. Analysis of the describing function diagram supports the former conclusion that a single 740Hz periodic orbit exists and is stable.

Now consider the phase portraits of the states which form the linear section of the delay-free model (x_1, x_2, x_3, x_4). These phase portraits display a strong stability in the large. That is all solutions head towards a limit set for sufficiently large initial conditions. Figure 7 shows the inner portion of a two-dimensional projection of the phase portrait for K=0.39. Notice

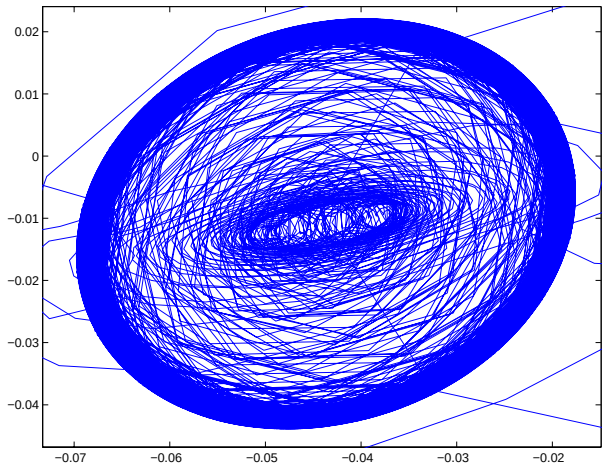

Figure 7: Zoomed phase portrait for states x_1 and x_2 with $K = 0.39$ and no noise.

that the attractor illustrates the 740Hz periodic orbit attractor (the dark outer ring), along with 210Hz resonant behavior which appears here as the inner structure. Our hypothesis is that this inner mode is actually a stationary orbit which is unstable. This second attractor at 210Hz stabilizes after a gain of K=0.64 is reached.

We see that, while the describing function analysis predicts the appearance of two periodic orbits for variations in the gain K, it is unable to forecast their stability. Bifurcation theory discusses the need to have some exchange of stability between branches of the bifurcation diagram. Simulation illustrates the detail. What we see at the identified gain of K=0.64 is that the 210Hz orbit is stable while the 740Hz orbit is hyperbolic, but survives as a stationary orbit with a nontrivial stable manifold.

4.4 Rapprochement with the data

Returning now to the data, we see that the two stationary orbits, 210Hz and 740Hz, are persistently represented in the data. So too is a small broad-band noise component. It is next logical to explore by simulation the behavior of the identified system with the inclusion of a small noise source adding into the loop. The spectrum of this response is illustrated in Figure 8 alongside that of the data. The concordance is remarkable, as is the ability of this modification to generate the persistence of both dominant spectral components. These observations reinforce the acceptability of the model but also dictate a desire for more stringent validation testing, not least because the identified gain differs from that needed to ensure good spectrum matching. To understand the behavior of this nonlinear system with two attractors excited by noise, we turn to the work of Knobloch and Weiss [KW89]. Subject to technical conditions on the attractors – "dissipativity" or phase

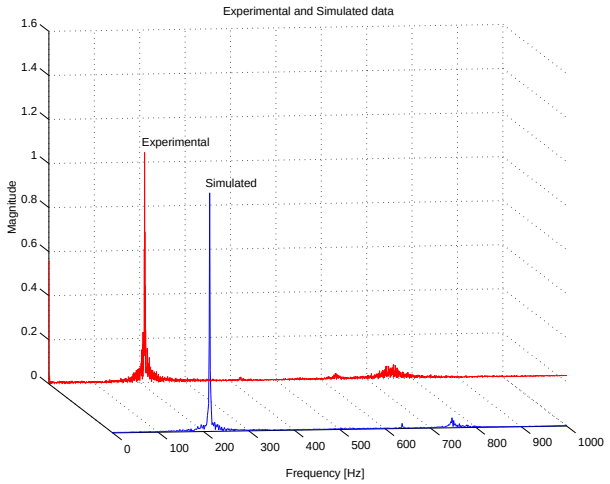

Figure 8: Experimental and simulated spectra of p_t. Simulation uses K=0.64, with noise added.

space volume contraction onto attractors – and on the noise – "fluctuation" or controllability from the noise input – the effect of the noise can be to force continuous transitions between the attractors which permit both frequencies to coexist.

Should the model be validated, then the satisfaction of these dissipation and fluctuation conditions (if then established) could provide a useful starting point for control design. However, at this stage we have simply provided evidence that this model could be capable of reproducing the experimental data. We have yet to test its predictive capability, since it is not feasible to alter the nonlinear gain occurring in the middle of the model.

5 Validation Experiment Design

The identification and simulation performed so far may spark some enthusiasm for the model. However we now seek to determine experiments to test more fully the proposed structure. In particular, our aims are to:
1. generate more information-rich signals within the loop in order that parameter identifiability be improved,
2. explore the appearance (or non-appearance) of qualitative dynamical phenomena as predicted by the existing structure and parameters,
3. derive from these tests model information which is useful for the subsequent design of feedback controllers.
Over-riding all of this is the requirement to provide guidance to the development of physically feasible experiments.

5.1 Physical Constraints

We need to consider how one might affect the loop signals by controlled external manipulation. The most attractive available source of actuation is through control of the fuel flow using a high-speed valve. This has the added advantage of exploring a likely control actuation mechanism simultaneously with the model validation. A typical limitation would be that fuel flow variations need to be small (say a few percent) and limited to less than 200Hz bandwidth (high frequency modulation of fuel injection is difficult to achieve reliably). This would modulate the equivalence ratio and should produce corresponding variations in the heat release rate q_t.

5.2 Experiment Design

Using fuel flow modulation and within the feasible region of signal bandwidth, we are restricted to a few types of signals for excitation of the limit cycling closed loop. Notably: single and multiple sinusoids, chirps, and band-limited noise, each at small signal amplitudes and each at frequencies neither too high (not feasible to actuate) nor too low (effectively alters the local equivalence ratio).

5.2.1 Band-Limited White Noise Injection:

The stochastic theory of [KW89] describes how the amount of noise perturbing a system affects the frequency of transitions between multiple attractors. With increased noise power, more time is shared between the attractors and the theory predicts that this would manifest itself in our model through the transfer of energy from the 210Hz mode to the 740Hz mode. Increasing the noise power by a factor of 10 over that used to generate Figure 8 produces the simulated system plot of Figure 9. Here we see that the magnitude of the limit

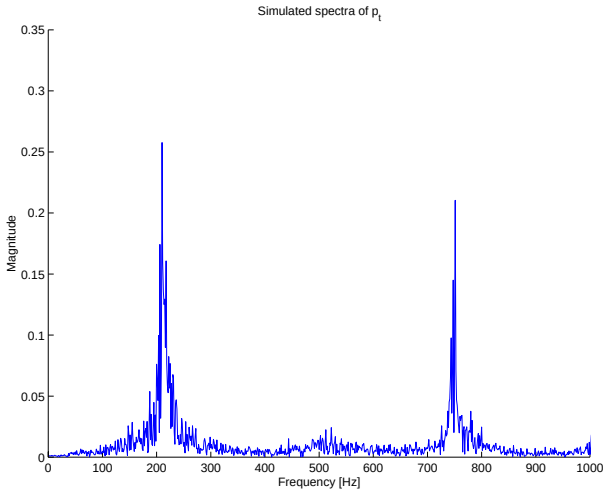

Figure 9: Simulated system with increased noise.

cycles is almost equal, indicating equal time spent on each attractor. This experiment has also widened the spectral content of the p_t, which would assist the quality of the identification process.

How this test might fare with band-limited noise injection is less certain. Although it is clear that the improvement of the spectral content should survive. With

small amplitude bandpass noise injected, smaller energy transfers are expected between the peaks. Casas [Casas99] has considered some approaches to the direct use of prediction error methods for the identification of parameters using such noise excited data.

5.2.2 Sinusoid and Chirp Injection: Figure 10 shows the spectrogram of the simulated pressure signal when a linear chirp is introduced additively into the heat release rate, q_t. The level of this chirp signal is 5% of the q_t signal and its range is from 50Hz to 200Hz over 0.8 seconds. At this rate of frequency change, the chirp effectively operates as a slowly scanning single-frequency sinusoid when compared to the number of cycles explored by the underlying attractors.

The spectrogram illustrates several features and masks some others. The interaction between the chirp and the attractors mostly occurs with the lower-frequency 210Hz attractor. The 740Hz oscillation increases in energy dramatically as well. The coupling between the chirp and the 210Hz depends very much on frequency but, typically, is a destructive interference until the signals coincide in frequency. The information content of the signals is improved.

With the injection of a single frequency sinusoid, these features become more pronounced and dependent upon the specific injection frequency. Thus injection at 45Hz almost extinguishes the 210Hz oscillation while injection at 50Hz has less effect. These are complex resonance phenomena. It is to be expected, however, that any feasible feedback control strategy would have to use phase-locked feedback between the pressure sensor and the fuel modulation.

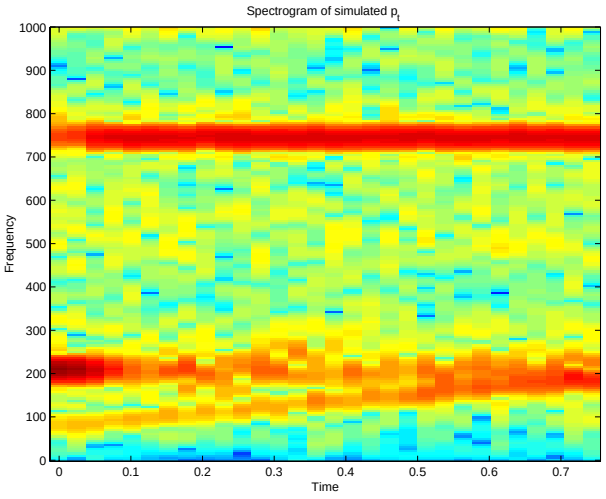

Figure 10: Spectrogram of simulated p_t with chirp input 50 to 200Hz and 5% of q_t.

With chirp and sinusoidal signals, one nonlinear effect was apparent: low level excitation of the system does not affect the dynamical properties of the oscillations. At q_t excitation signal levels below about 4% there was no appreciable change to the simulated loop signals. Above this level, those effects indicated above became apparent. One could speculate on the information that this might give about the separation between attractors. But this is premature. With multiple sinusoidal excitation signals, it becomes more difficult to discern a useful structure to the response.

6 Conclusions

Validation experiment design for this class of nonlinear combustion models uses nonlinear dynamical system methods to analyze the expected behavior of the system under injection of bandpass signals. The recommended feasible approach is to use chirp excitation above 4% of the fuel flow from about 50Hz to 200Hz. The validation test is to detect the energy transfer between modes of the system.

References

[SBD2K] S.M. Savaresi, R.R. Bitmead and W.J. Dunstan, "Nonlinear System Identification of a Closed-loop Lean Combustion Process," *IFAC Symposium on System Identification*, Santa Barbara, USA, 2000.

[PP98] A.A. Peracchio and W.M. Proscia, "Nonlinear Heat-release/Acoustic Model for Thermoacoustic Instability in Lean Premixed Combustors," *ASME/IGTI Turbo Expo*, Stockholm, Sweden, 1998.

[MJC+98] R.M. Murray, C.A. Jacobson, R. Casas, A.I. Khibnik, C.R. Johnson Jr, R.R. Bitmead, A.A. Peracchio and W.M. Proscia, "System Identification for Limit Cycling Systems: a Case Study for Combustion Instabilities," *American Control Conference,* Philadelphia, USA, pp. 2004-2008, 1998.

[KW89] E. Knobloch and J.B. Weiss, "Effect of Noise on Discrete Dynamical Systems with Multiple Attractors," in *Noise in Nonlinear Dynamical Systems, Vol. 2: Theory of noise induced processes in special applications,* F. Moss and P.V.E. McClintock (eds), Cambridge University Press, pp. 65-86, 1989.

[Casas99] R.A. Casas, *Identification of Nonlinear Feedback Systems Operating in Limit Cycle,* Ph.D. dissertation, Cornell University, Ithaca, USA, 1999.

[GH96] J. Guckenheimer, P. Holmes, *Nonlinear Oscillations, Dynamical Systems, And Bifurcations Of Vector Fields* New York : Springer-Verlag, 1983.